Optimum design for BB84 quantum key distribution in tree-type passive optical networks

José Capmany,[1,*] and Carlos R. Fernández-Pousa[2]

[1] ITEAM Research Institute, Universidad Politécnica de Valencia, 46022 Valencia, Spain

[2] Signal Theory and Communications, Dep. of Physics and Computer Science, Univ. Miguel Hernández, 03202 Elche, Spain

[*]Corresponding author: jcapmany@iteam.upv.es

We show that there is a tradeoff between the useful key distribution bit rate and the total length of deployed fiber in tree-type passive optical networks for BB84 quantum key distribution applications. A two stage splitting architecture where one splitting is carried in the central office and a second in the outside plant and figure of merit to account for the tradeoff are proposed. We find that there is an optimum solution for the splitting ratios of both stages and then analyze the effects of the different relevant physical parameters of the PON on the optimum solution.

OCIS codes: (030.5260) Photon counting; (040.5570) Quantum detectors; (060.0060) Fiber optics and optical communication; (270.0270) Quantum optics.

1 Introduction

The objective of Quantum Key Distribution (QKD) is to provide an unique way of sharing a random sequence of bits between users with a level of security not attainable with either public or secret-key classical cryptographic systems [1,2]. In essence, QKD relies on exploiting the laws of quantum mechanics [3,4]. Most of the reported experimental results on long distance QKD rely on different photonic-based techniques and are based on the so-called BB84 protocol. For instance, in 1992 Bennett and co-workers [5] proposed to exploit the polarization of photons to implement the four required states by employing one circular polarization and one linear polarization basis. Later, Townsend and co-workers [6-8], proposed the use of optical delays and balanced interferometers at the transmitter and the receiver. A third approach, based on differential phase shift quantum key distribution [9] has enabled key generation and distribution along distances over 100 Km [10] although with limited security, [11]. Finally, a fourth approach [12], also known as frequency coding, relies on encoding the information bits on the sidebands of either phase [13] or amplitude [14], radio-frequency (RF) modulated light.

Much of the work reported in the literature has been focused towards point to point key distribution but, as pointed in [7],[15], to find truly widespread application QKD techniques should be employed in communication networks where any-to-any and any-to many transmission can occur. In particular, a first scenario where this may happen is in fiber based passive optical networks, where the passive nature (no optical amplification) and the limited distance range (up to 20 Km) favors the implementation of multiuser BB84 QKD systems. In this context, recent contributions [16] have addressed the comparison of different multiuser quantum key distribution schemes over PONs, paying especial emphasis on the attainable quantum bit error rate QBER but not addressing the issue of combined QBER or even more important, useful

key distribution bit rate and resource optimization which even in the most simple PON configurations cannot be considered as uncoupled factors. To illustrate this point, the upper part of figure 1 shows a typical N-user tree-PON configuration where Alice, at the central office is connected via an optical fiber link of length L_1 to a *1XN* passive splitter.

Each of the *N* outputs of the splitter connects to a different end-user (Bob_i, $i=1, 2...N$) via an optical fiber link of length L_2 (we will assume that the length of any Alice-Bob_i connection is fixed and equal to $L=L_1+L_2$). As discussed elsewhere [15], the quantum level behavior of the splitter enables the key distribution task between Alice and the different Bobs, since a single photon incident on the splitter cannot be divided, but it will be randomly (and unpredictably) routed to one (and only one) of the output paths, with a probability given by *1/N*. If we assume that Alice and the different end-users employ a BB84 protocol for key distribution, based on any of the above reported photonic techniques, then it is easy to compute the end-to-end power transmission factor of a particular Alice-Bob_i connection, which is given by $T_L = e^{-\alpha L} / N$, where α is the fiber attenuation constant. Also, we can have an estimation of the optical resources employed by calculating the total length of deployed fiber in the PON, which is given by $L_T = L_1 + NL_2$. To improve the power transmission factor one could think, for instance, in including the *1xN* splitter inside the central office as shown in the lower part of figure 1. In this case, the power transmission factor is increased by a factor of *N*, that is, $T_L = e^{-\alpha L}$, but the total length of deployed fiber in the PON is increased up to $L_T = NL_1 + NL_2 = NL$. Thus, as it can be appreciated, increasing the end-to-end transmission factor (and thus decreasing its QBER and, in consequence, the useful key distribution bit rate R_{net}) of a given Alice-Bob_i connection comes at the price of requiring higher hardware resources. There is thus a design tradeoff between R_{net} and deployed fiber length in the tree-type PON, for which we wish to find an optimum solution.

The purpose of this paper is to find such a solution and discuss the effect of the different and relevant physical parameters of the BB84 QKD system on it.

2 Tree PON Architecture Description

Figure 2 shows the proposed two splitting stage PON layout that is an intermediate case between the two previously discussed. Here, a first $1XN_1$ passive splitter is located inside the central office at the output of Alice's transmitter and thus it does not contribute to the PON's loss. A different fiber link of length L_1 connects each of the outputs from the $1XN_1$ splitter to an $1xN_2$ secondary splitter which, in turn, is connected by different fiber links of length L_2 to N_2 different final users (Bob_i, i=1,2..N). We assume that Alice's transmitter and Bob_i's (i=1,2,…N) are the required for the particular encoding method employed to implement the BB84 protocol (polarizations, phase or frequency).

Referring to figure 2 the end to end transmission from Alice to a particular Bob_i due to system's losses are given by:

$$T_L = \frac{e^{-\alpha(L_1+L_2)}}{N_2} = \frac{T_F}{N_2} = \frac{N_1 T_F}{N} \tag{1}$$

While the total length of fiber employed to connect the final users to Alice is given by:

$$L_T = N_1 L_1 + N L_2 \tag{2}$$

Note that N_1 and N_2 are linked by the relationship $N=N_1.N_2$, where N is the total number of end users. Increasing the value of N_1 (and thus decreasing the value of N_2) results in lower end-to end transmission losses but an increase in the total length of deployed fiber in the PON.

Conversely, increasing the value of N_2 (and thus decreasing the value of N_1) results in higher end-to end transmission losses and a decrease in the total length of deployed fiber in the PON.

The values given by (1) and (2) lie in between those of the two extreme cases that we considered in the introduction section which optimize, respectively, the total length of fiber deployed and the end-to-end loss. Since there is a trade-off between both parameters it is our aim to find an optimum configuration that can balance both contributions.

3 QKD Network Figure of Merit and Optimization

For optimization of the PON configuration we need a figure of merit that can take into account both the effects of transmission losses and the total length of fiber deployed. Since the first directly impacts the QKD performance via the quantum bit error rate (QBER) and therefore the useful key distribution bit rate R_{net} we propose the following expression:

$$FOM = \left(\frac{R_{net}}{L_T} \right) \tag{3}$$

Here, the useful key distribution bit rate R_{net} is connected to the quantum bit error rate by [3]:

$$R_{net} = R_{sift} \left[1 + QBER \log_2(QBER) + (1 - QBER) \log_2(1 - QBER) - \frac{2}{Ln2} QBER \right] \tag{4}$$

Where R_{sift} is the bit rate of the sifted key. It can be immediately checked that an increase in *QBER* results in a decrease of R_{net} and viceversa. The reader can check that (3) is consistent with the trade-off previously described, since an increase in the total length of the deployed fiber reduces the *FOM* through the inverse dependence with L_T but, at the same time, since end to end transmission losses are decreased (N_2 decreases) then so does the value of the QBER (and

therefore R_{net} increases), hence, the R_{net} factor tends to increase the FOM. On the other hand, a decrease in the total length of deployed fiber increases the FOM value through the $(1/L_T)$ factor, while the increase in N_2 decreases the FOM through the R_{net} factor.

We can further develop the expression of the FOM showing its explicit dependence on N_1 by substituting (2), (4) into (3) and using the standard QBER expression for BB84 systems which can be found elsewhere [3], [16]:

$$FOM = \frac{R_{sift}\left[1 + QBER(N_1)\log_2(QBER(N_1)) + (1 - QBER(N_1))\log_2(1 - QBER(N_1)) - \frac{2}{Ln2}QBER(N_1)\right]}{(N_1 L_1 + NL_2)}$$
$$QBER(N_1) = \frac{(\mu\eta N_1 T_F(1 - V) + Nd_B)}{2\mu\eta N_1 T_F} \quad (5)$$

In the above expression V represents the optical visibility achieved in the filtering process, η the detector efficiency, μ is the average photon number at the output of Alice's transmitter and d_B is the dark count rate.

We now optimize the FOM with respect to the branching ratio N_1 in the central office splitter:

$$\frac{\partial FOM}{\partial N_1} = 0 \Rightarrow$$
$$\Rightarrow \frac{Nd_B(N_1 L_1 + NL_2)}{2\mu\eta N_1 T_F}\left[Ln(QBER(N_1)) - 2\right] + N_1^2 L_1\left[Ln(2) + QBER(N_1)Ln(QBER(N_1)) - 3QBER(N_1)\right] = 0 \quad (6)$$

Eq.(6) is an implicit equation in N_1 that must be solved numerically and from which we can analyze the role that the different parameters play on the network design.

4 Results and Discussions

The effects of the different physical parameters on the optimum design of the branching ratios of the tree-PON architecture can be now investigated with the help of Eq.(6). Unless stated otherwise, we have taken the following typical values for $\lambda=1550nm$: $d_B=10^{-5}$, $\mu = 0.1$, V=0.98, $\eta = 0.1$, $L=L_1+L_2=20Km$, $\alpha=0.25dB/Km$. A first caution which has to be taken when using Eq.(6) is that it does not render integer values. Since optical splitters provide an integer number of output ports the results given by Eq.(6) have to be approximated taking into account the type of division provided by the splitters. Although *1x3, 1x5, 1x7* splitters are commercially available, we have chosen for our simulations splitters of the type $1x2^I$, where $I=0,1,2,3$….since these are the most commonly available in the market. Figure 3 shows the evolution of the optimum value of N_1 in terms of L_1, the link length of the first stage for a PON serving $N=32$ users. The values given directly by Eq.(6) (blue trace) and by its approximation, when considering multiple of 2 branching splitters (red trace), are depicted.

Both curves show a similar qualitative behavior. N_1 decreases as the length L_1 of the first stage in the PON increases as expected since for low values of L_1 the contribution of the first stage to the total length of deployed fiber is less significant. Then, according to the discussion in section 1, N_1 should be close to N. Note that the decrease in the value of N_1 with L_1 is nonlinear as anticipated by the implicit nature of Eq.6. We next discuss the behavior in terms of the number of users served by the tree PON. Figure 4.a shows the evolution of the optimum value of N_1 in terms of L_1, for different values of the total number of users ($N=8,16,32,64,128$).

A similar behavior is observed in all the cases with a decreasing behaviour as L_1 is increased. Figure 4.b shows as well the computed value for the R_{net}/R_{sift} ratio and the QBER values for the case where the number of users is the highest (128) and so the expected splitting

losses. Note that for this particular configuration despite the maximum QBER values are confortably below the 15% limit reaching a maximum of around 5.7% the R_{net}/R_{sift} ratio can considerably decrease up to a 53%, thus it is this performance quantity and not the QBER which has to be considered when addressig the design of the nwtwork. Figure 5.a shows the evolution of the optimum value of N_1 in terms of L_1, for different values of the mean number of photons μ in the weak coherent pulses at Alice´s output. For a given value of L_1 Eq.(6) yields an increase in the value of N_1 for decreasing values of μ. This is due to the fact that when μ increases the end-to-end transmission factor increases (i.e. the QBER decreases or alternatively, R_{net} increases). Thus, the same end-to-end performance can be achieved with a lower value of N_1. The value of value for the R_{net}/R_{sift} ratio as a function of L_1 is plotted in figure 5.b. As expected, this value is more tolerant to variations in L_1 for higher values of the mean number of photons μ.

Finally, we examine the effect of the operating spectral window on the optimum N_1 value. We consider the case of a PON serving 32 users and two different cases $\lambda=1550\ nm$ and $\lambda=1300\ nm$. For this last case both the attenuation coefficient and the typical photodetector efficiency must be changed ($\alpha=0.35dB/Km,\ \eta=0.2$) . The results are plotted in figure 6. For a fixed value of L_1 operation in the second window requires, in general, a lower splitting ratio. This is due to the fact that the product ηT_F is higher at 1300 nm than at 1550nm, mostly beacuse of the increase in the value of the detector efficiency.

5 Summary and Conclusions

In summary, we have shown that there is a tradeoff between useful key distribution bit rate R_{net} and the total length of deployed fiber in tree-type passive optical networks for BB84 quantum key distribution applications. We have proposed a two stage splitting architecture where one

splitting is carried in the central office and therefore does not conribute to system's loss and a second in the outside plant. We have proposed and justified a figure of merit to account for the tradeoff and found that there is an optimum solution for the splitting ratios of both stages. We have then analysed the effects of the different relevant physical parameters of the PON in the optimum solution.

Acknowledgements

The authors wish to acknowledge the financial support of the Spanish Government through Quantum Optical Information Technology (QOIT), a CONSOLIDER-INGENIO 2010 Project and the Generalitat Valenciana through the PROMETEO research excellency award programme GVA PROMETEO 2008/092.

References

1. S. Wiesner, “Conjugate coding”, SIGACT News **15**, 77-88 (1983).
2. C. H. Bennett and G. Brassard, “ Quantum cryptography: Public key distribution and coin tossing” in Proceedings of the IEEE International Conference on Computers, Systems and Signal Processing, Bangalore, India, 1984 IEEE, New York, 175-179 (1984).
3. N. Gisin, G. Ribordy, W. Tittel, and H. Zbiden, “Quantum Cryptography”, Rev. Mod. Phys. **74**, 145-195 (2002).
4. W. K. Wootters and W. H. Zurek, “A single quantum cannot be cloned”, Nature London, **299**, 802-803 (1982).
5. C. H. Bennett, F. Bessette, G. Brassard, L. Salvail, and J. Smolin, “Experimental quantum cryptography”, J. Cryptology **5**, 3 (1992).
6. P. D. Townsend, J. G. Rarity, and P. R. Tapster, “Single-photon interference in a 10 Km long optical fiber interferometer”, Electron. Lett. **29**, 634-635 (1993).
7. P. D. Townsend, D. J. D. Phoenix, K. J. Blow and S. Cova, “Design of quantum cryptography systems for passive optical Networks”, Electron. Lett. **30**, 1875-1876 (1994).
8. P. D. Townsend, “Quantum Cryptography on Optical fiber networks”, Opt. Fiber Technol. **4**, 345-370 (1998).
9. K. Inoue, E. Waks and Y. Yamamoto, “Differential phase shift quantum key distribution”, Phys. Rev. Lett. **89**, (037902) (2002).
10. H. Takesue, E. Diamanti, T. Honjo, C. Langrock, M. M. Fejer, K. Inoue and Y. Yamamoto, “Differential phase shift quantum key distribution over 105 km fibre”, New J. Phys. **7**, 1-12 (2005).

11. M. Curty, K.Tamaki and T. Moroder, “Effect of detector dead times on the security evaluation of differential-phase-shift quantum key distribution against sequential attacks”, Phys Rev. A, **77** (052321) (2008).
12. J-M. Mérolla, Y. Mazurenko, J. P. Goedgebuer, and W. T. Rhodes, “Single-photon interference in Sidebands of Phase-Modulated Light for Quantum Cryptography”, Phys. Rev. Lett. **82**, 1656-1659 (1999).
13. J-M. Mérolla, Y. Mazurenko, J. P. Goedgebuer, H. Porte, and W. T. Rhodes, “Phase-modulation transmission system for quantum cryptography”, Opt. Lett. **24**, 104-106 (1999).
14. O. Guerreau, J-M. Mérolla, A. Soujaeff, F. Patois, J. P. Goedgebuer, and F. J. Malassenet, “Long distance QKD transmission using single-sideband detection scheme with WDM synchronization”, IEEE J. Sel. Top. Quantum Electron. **9**, 1533-1540 (2003).
15. P.D. Townsend, “Quantum cryptography on multi-user optical networks”, Nature, **385**, 47-49 (1997)
16. P.D. Kumavor, A.C. Beal, S. Yelin, E. Donkor and B.C. Wang, “Comparison of four multi-user quantum key distribution schemes over passive optical networks’, IEEE J. Lightwave Technol., **23**, 268-276 (2005)

Figure Captions

Figure 1. Two tree-PON configurations for BB84-QKD. In the upper configuration the 1xN splitter affects the end-to end power transmission (and the QBER) between Alice and Bobi but minimum fiber resources need to be deployed. In the lower configuration the 1XN splitter does not affect the QBER but maximum fiber resources need to be deployed .

Figure 2. Proposed two-splitting-stage PON.

Figure 3. Evolution of the optimum value of N_1 in terms of L_1, for a PON serving 32 users.

Figure 4.a. Evolution of the optimum value of N_1 in terms of L_1, for a PON serving 8,16,32,64 and 128 users.

Figure 4.b. Evolution of the optimum value of the useful key distribution bit rate (normalized to the sifted key bit rate) and the QBER in terms of L_1, for a PON serving 128 users.

Figure 5.a. Evolution of the optimum value of N_1 in terms of L_1, for a PON serving 32 users for different values in the mean output photons in the weak coherent pulses at Alice's output.

Figure 5.b. Evolution of the optimum value of the useful key distribution bit rate (normalized to the sifted key bit rate) in terms of L_1, for a PON serving 32 users for different values in the mean output photons in the weak coherent pulses at Alice's output.

Figure 6. Evolution of the optimum value of N_1 in terms of L_1, for a PON serving 32 users for different operation wavelengths.

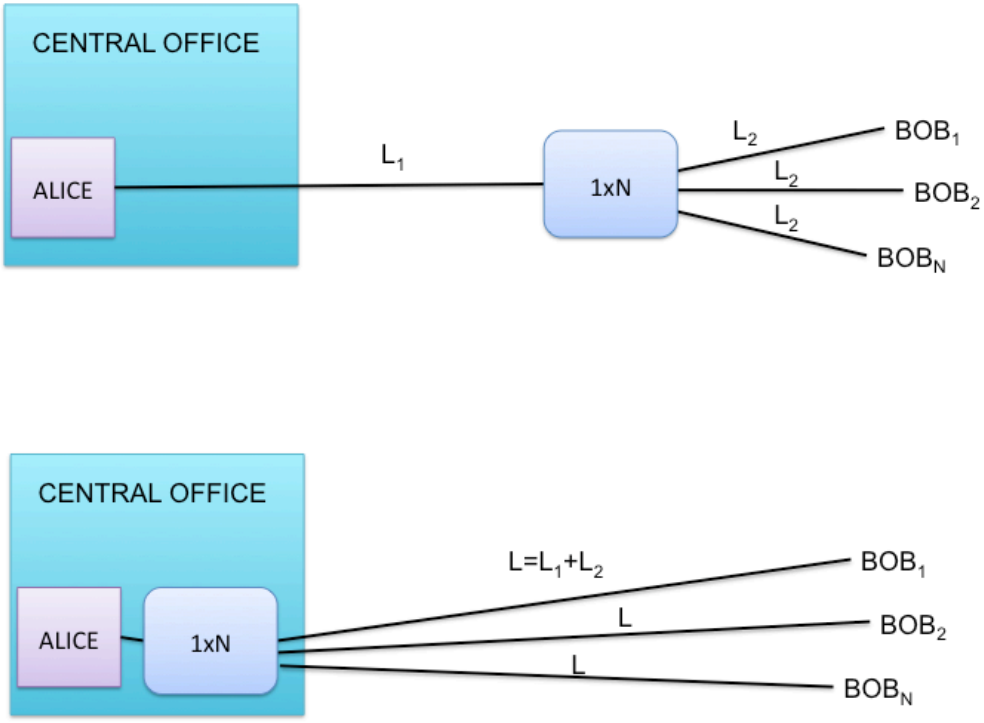
CENTRAL OFFICE
ALICE
L1
1xN
L2
L2
L2
BOB1
BOB2
BOBN
CENTRAL OFFICE
ALICE
1xN
L=L1+L2
L
L
BOB1
BOB2
BOBN

FIGURE 1

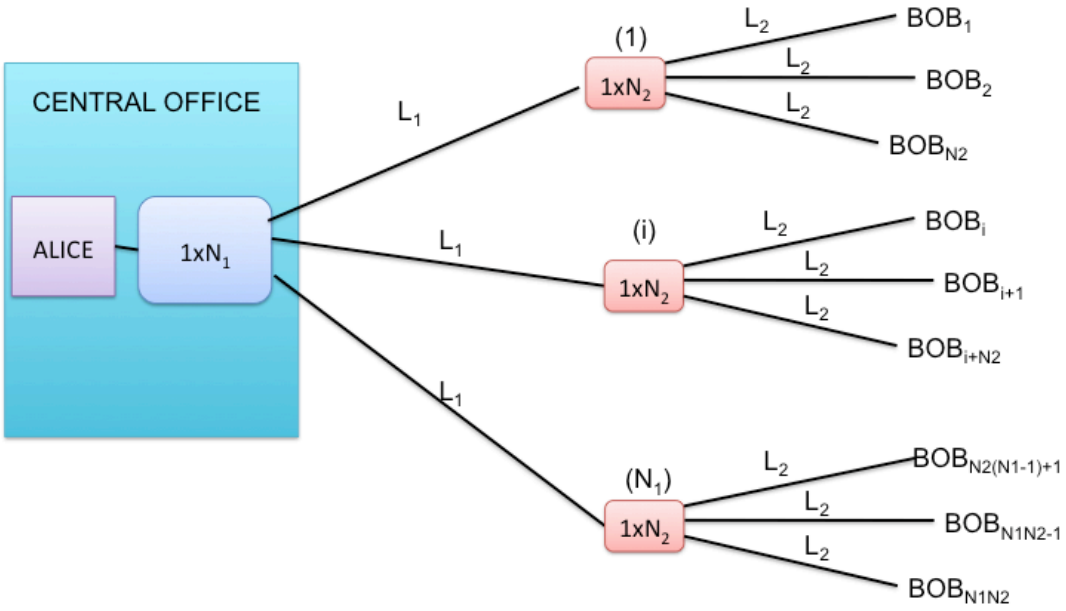
CENTRAL OFFICE
ALICE
1xN1
L1
L1
L1
(1)
1xN2
(i)
1xN2
(N1)
1xN2
L2
L2
L2
L2
L2
L2
L2
L2
L2
BOB1
BOB2
BOBN2
BOBi
BOBi+1
BOBi+N2
BOBN2(N1-1)+1
BOBN1N2-1
BOBN1N2

FIGURE 2

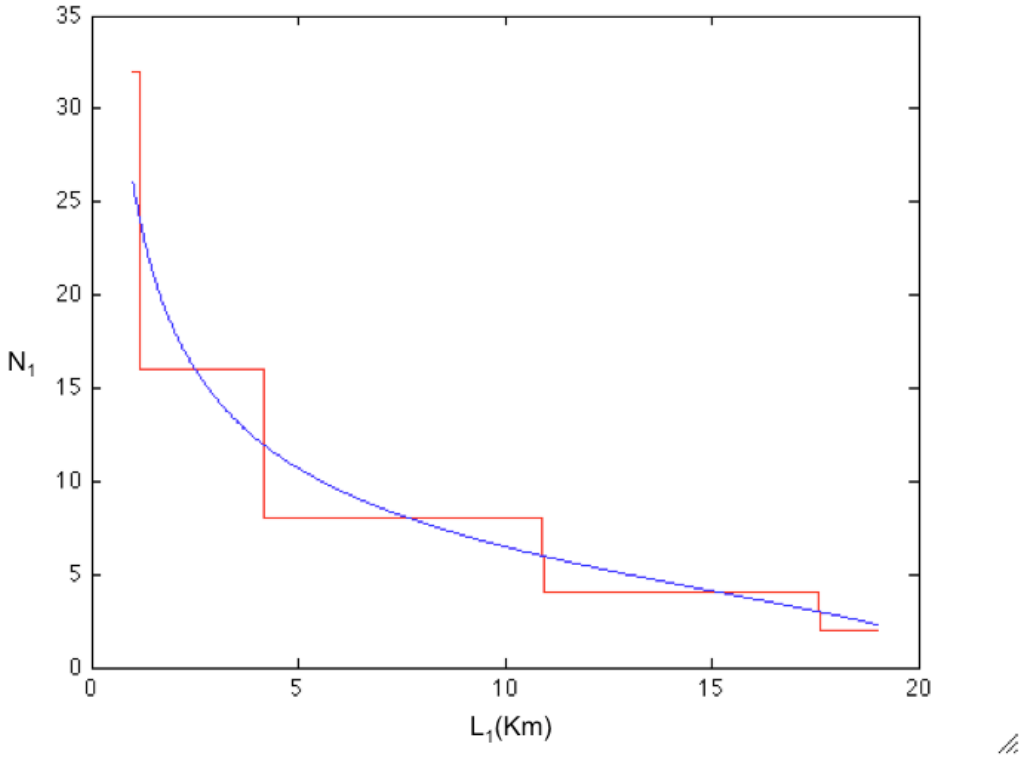

FIGURE 3

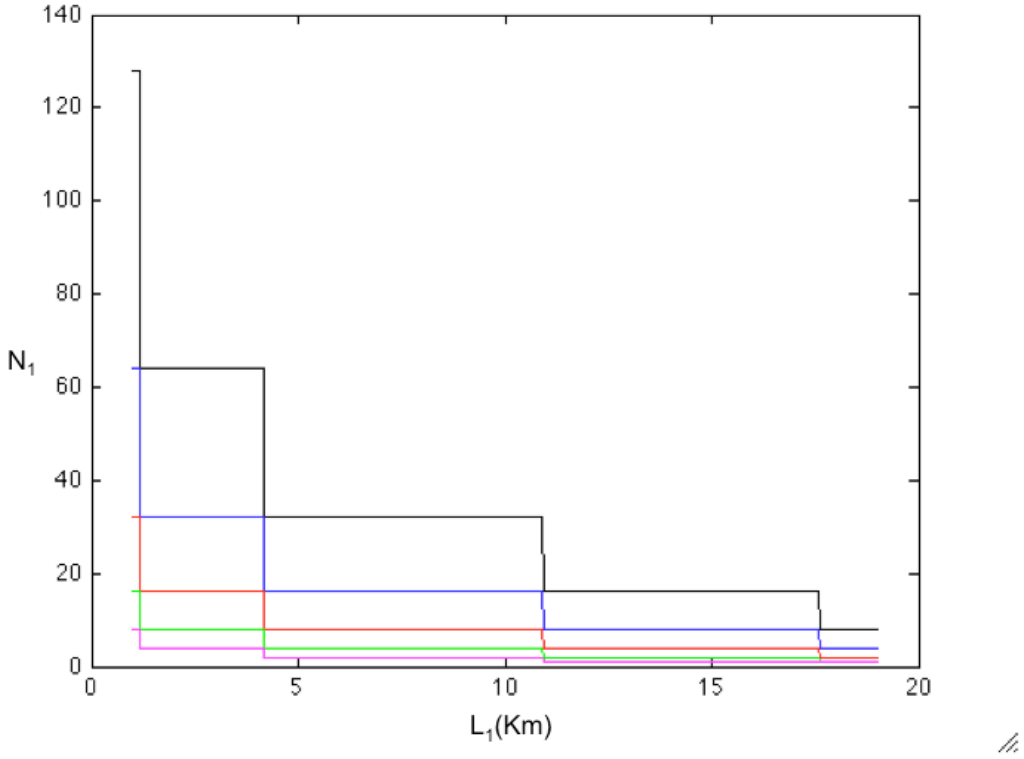

FIGURE 4.a

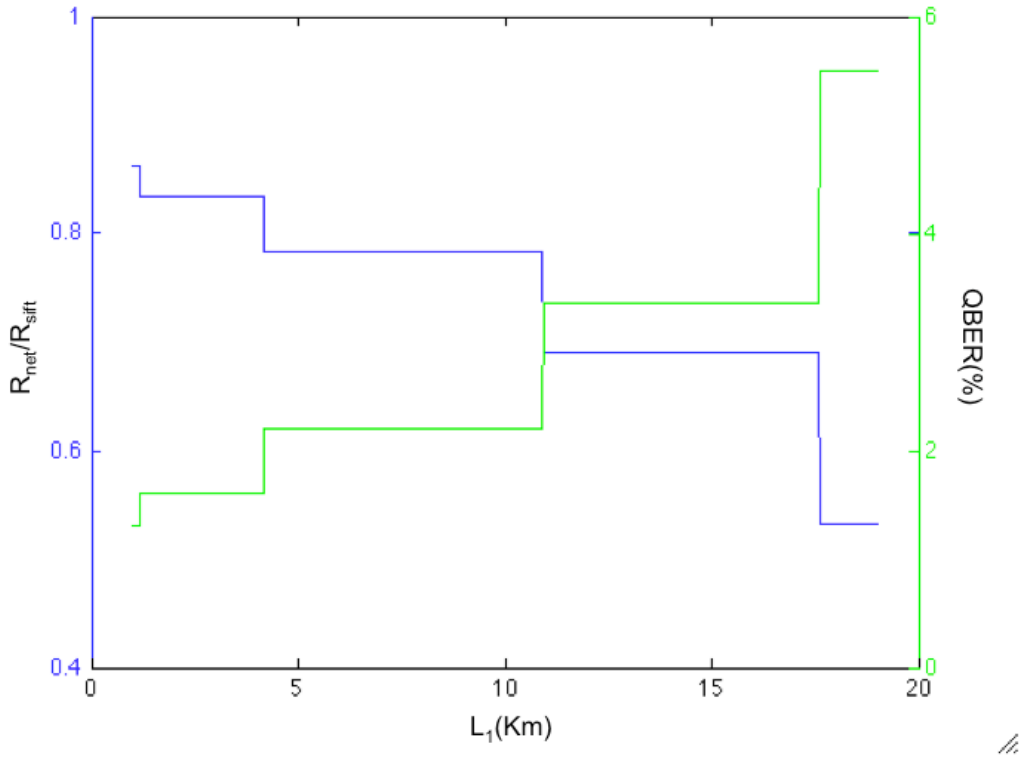

FIGURE 4.b

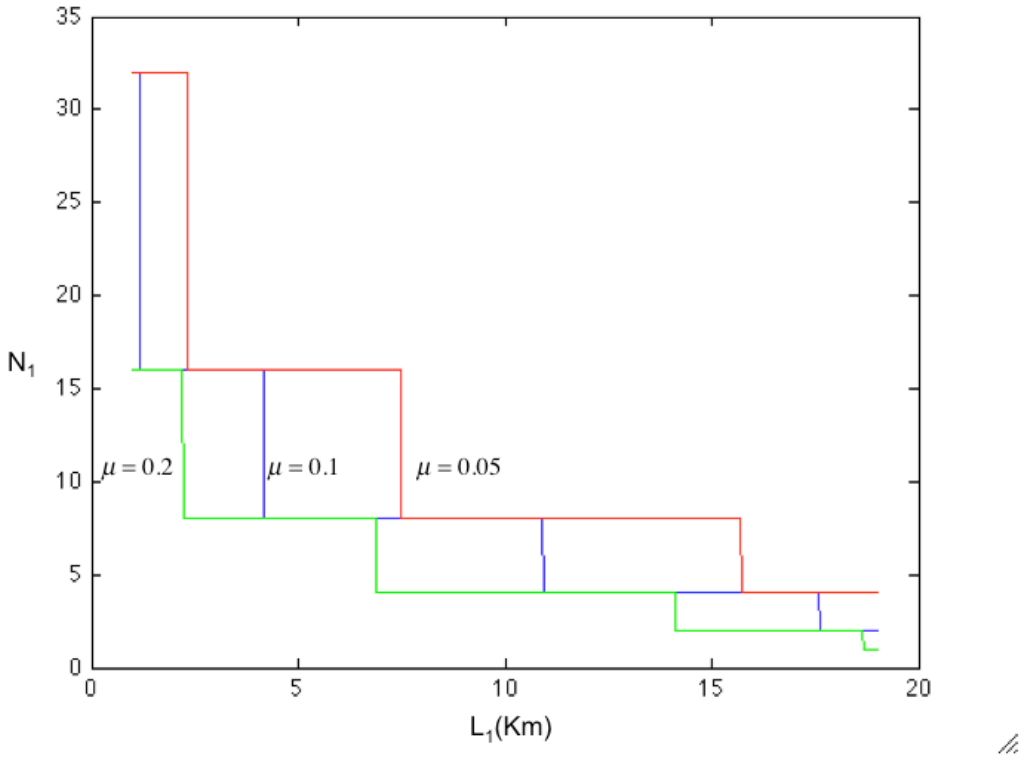

FIGURE 5.a

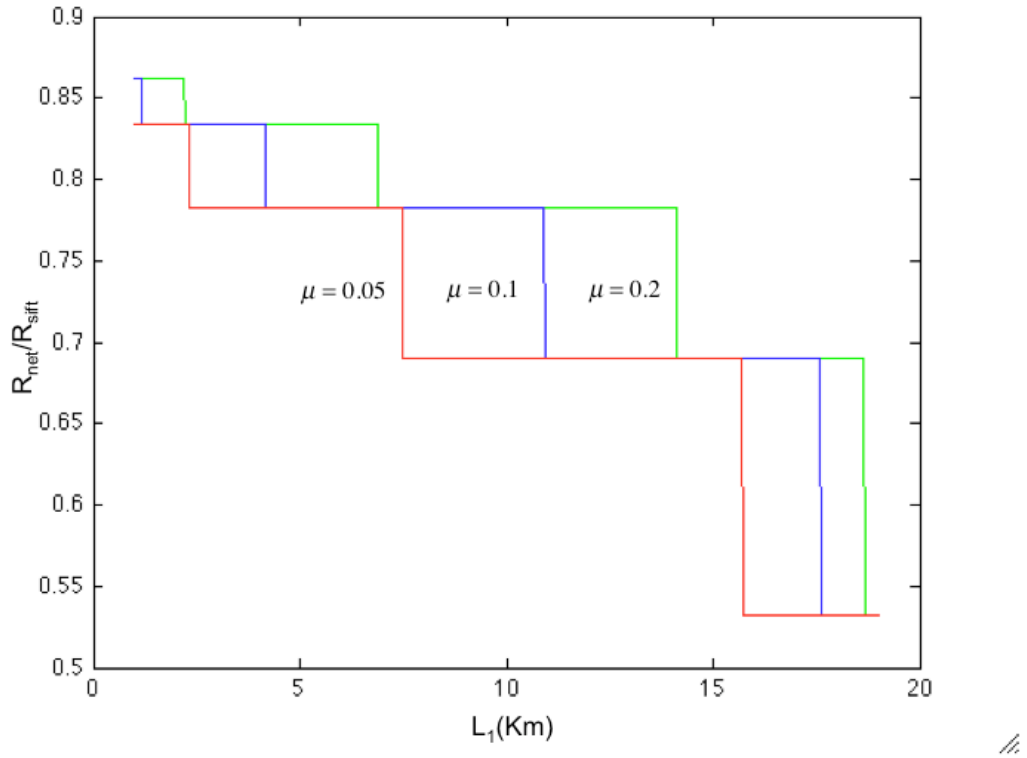
0.9
0.85
0.8
0.75
0.7
0.65
0.6
0.55
0.5
0
5
10
15
20
R_{net}/R_{sift}
L_1(Km)
$\mu = 0.05$
$\mu = 0.1$
$\mu = 0.2$

FIGURE 5.b

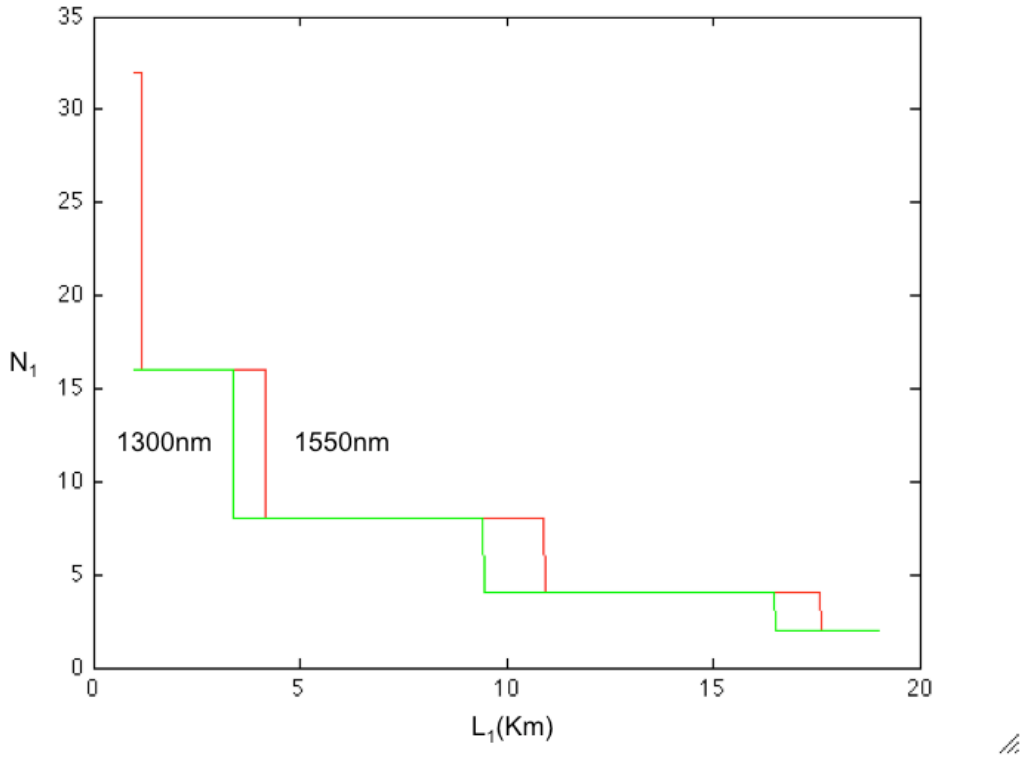

FIGURE 6